Synthesis of zinc oxide-goethite composite and its performance on the adsorption of arsenite in aqueous media.

Egirani DE[1]*, Poyi NR[2], Wassey N[1]

[1]Niger Delta University, Wilberforce Island, Nigeria
[2]Nigerian Institute of Mining and Geosciences, Jos, Nigeria

Abstract

This paper investigated the synthesis of Zinc oxide-Pary Mountain Mine (PMM)-goethite composite and its performance in the adsorption of arsenite. The trimetric approach was used in the synthesis and characterization was carried out using usual laboratory procedures. Batch mode techniques at ambient temperature were used to test the adsorption of arsenite on zinc oxide PMM coated goethite. The mechanism of the reaction indicated less than one proton coefficient of 0.74, an intraparticle diffusion that was controlled by a boundary layer with a slope of 1.13^{-3} (mg^{-1}) min$^{0.5}$, and an intercept C that was 9.96. The mass transfer rates were 3.608^{-6} cm^{2}hr^{-1}, 1.958^{-6} cm^{2}hr^{-1} and 0.7521^{-6} cm^{2}hr^{-1}. There was an enhancement of the mass transfer of adsorbate to the external layer of the adsorbent. The capacity of adsorption increased with increase in contact time. The first part of the linear plot may be linked to larger numbers of active adsorption sites. The aging reaction provided the different magnitude of adsorption capacity. Based on pH variability, the adsorption efficiency of the zinc oxide-goethite composite was 93.05%.

Introduction

The aquatic environment is the biggest recipient of arsenic ions in both organic and inorganic forms. The inorganic forms (i.e. arsenite and arsenate predominate over other forms in the ecosystem [1,2]. Arsenic is toxic and its presence in drinking water constitutes a problem to humans and the ecosystem [3-5]. Inorganic arsenic species are strong carcinogens to humans [6-8]. The toxic effect of arsenic varies from skin lesions, disturbance of the nervous system to the destruction of vital organs of the human body, thus leading to death [9,10]. Therefore, the international and regional regulators have reduced the arsenic standard concentration in drinking water to 10 µgL^{-1} [11]. The use of bare goethite in the treatment of arsenic contaminated aqueous environment formed the subject of previous studies under the same experimental conditions [12-17].

In this study, an emerging technique for the removal of arsenic from hydrometallurgical waste has been discussed. The release of hydrometallurgical waste to the aquatic environment constitutes a modern source of arsenic in groundwater. This contamination is through infiltration into shallow wells [18]. The hydrometallurgical treatment of sphalerite to extract zinc metal generates slurries and leaching muds. These wastes contain zinc oxide, hydrated iron oxide, and impurities of arsenic, antimony, and germanium. Due to acid treatment, the pH of these slurries and leaching muds is usually less than 5. Before discharge into the aquatic environment, they are stored in sealed plastic tanks under reducing condition. This process stimulates the lowering of the concentration of metals and metalloid in the slurries and leaching muds [19]. The oxidation-reduction state of these metallurgical wastes has a substantial effect on the leaching of elements. Under the reducing condition, leached out metals and

compounds including ZnO-goethite interface will be negligible [20] The Eh-pH diagram of arsenic species as reported by Masscheleyn PH, Delaune RD and Patrick Jr WH [21] supported that arsenite exists in acid pH under reducing condition. In addition, reduction of arsenate to arsenite is possible in this pH range and under reducing condition. Therefore, there is a need to mimic in the laboratory the removal of arsenite from hydrometallurgical contained-wastewater.

There are controlling factors and emerging techniques in the removal of arsenic from the aquatic environment. Dissolved arsenic species at low concentrations are controlled by the concentration of adsorbent and chemistry of solutions [22]. In addition, the contact time and solution pH are factors which regulate the hydrolysis of arsenic ions and species [23]. Aluminum-Coated goethite reduces adsorption. The available surface area and surface-active sites control arsenic uptake. The contact time or aging enhances the reorganization of mineral surfaces in aqueous solution [24].

The reaction mechanism involving four steps of mass transfer has been described to arsenite removal in aqueous solution. These mechanisms include the film surrounding the adsorbent as the recipient of adsorbate, the surface of adsorbent as the recipient of adsorbate, intraparticle diffusion and adsorbent sites as the recipient of adsorbate. Here, the Weber and Morris intraparticle diffusion model was used to support the reaction mechanism [25]. The fast process of intraparticle diffusion and slow process of outer-sphere complexation are components of the reaction mechanism involved in arsenic uptake in aqueous solution. In addition, solution dilution and exchange stoichiometry control the removal of arsenite from the aquatic environment [12,14]. Some of the successive steps identified as ways for a solid-solution system, undergoing adsorption include

external mass transfer, intra-particle diffusion, protonation and adsorption of molecules of adsorbate [26] Therefore, the use of kinetic models to depict the reaction mechanism involved in arsenite removal is necessary.

The conservative methods used in the treatment of arsenic contaminated water include adsorption, chemical precipitation, and electrochemical recovery. In addition, some reviews involving arsenic adsorption have been done. However, the rather expensive techniques for limited size water treatment systems demand the sourcing of innovative cost-effective treatment processes. In consideration of cost and design simplicity, adsorption is taken as a simple technique for treatment of water [27,28].

In this article, the effect of zinc oxide-goethite composite on arsenite removal has been studied in comparison with the previous studies. This was in relation to pH, contact time, arsenite initial concentration, and aging. This study was aimed at mimicking the role of synthetic and characterized zinc oxide coated goethite in the treatment of arsenic contaminated slurries and leaching muds in the metallurgical industry. This follow-up study was aimed at providing evidence that the presence of synthetic zinc oxide-goethite composite enhanced arsenite adsorption. Batch mode experimental techniques under reducing condition, were used to carry out the experiments in relation to the variables under consideration. Synthesis of the adsorbent, characterization of the system and the testing of zinc oxide-goethite composite to remove arsenite have been discussed.

Materials and Experimental Methods

Materials and reagents

All reagents used were of analytical grade. The PMM goethite was collected from settling ponds at Parys Mountain mine in Anglesey, United Kingdom. The yellow amorphous ferric hydrous oxide precipitate was sieved to 100 µm and washed with double distilled water. Merck Company from Germany provided the arsenite stock solution. A Titrisol ampule with As_2O_3 in H_2O in a volumetric flask was used to prepare the AAS standard solution of 1000 mgL^{-1} arsenite. As instructed by Merk guidelines, the content after filling up to mark was securely sealed and kept in the dark to avoid oxidation. The working solutions of different concentrations were provided by diluting the stock solution. In addition, the zinc nitrate used as the precursor and KOH used as the precipitating agent were purchased from Sigma-Aldrich (Belgium).

Preparation of anaerobic suspensions

To create a reducing condition for all experimental content, all solutions were prepared using water that has been de-aerated and deionized. Deionized water was obtained from a Millipore Milli-Q system (18.2 MΩ.cm at room temperature). The experimental content was bubbled through continuously for 24 h using purified nitrogen gas. The content was securely sealed and stored in airtight containers in the anaerobic chamber in the dark before use [14].

Adsorbent characterization

The PMM goethite contained SiO_2 (0.30%), Al_2O_3 (17.00%), FeO (62.62%), CaO (0.23%), MgO (0.03%), K_2O (0.02%),

and 0.06% MnO. These elements were determined using X-ray fluorescence. The pH of PMM goethite suspension was 3.00, and pH of the reacting solutions were evaluated using the Model 3340 Jenway ion meter. The external surface area of the PMM goethite and ZnO-goethite composite (97.00 m^2/g and 458.15 m^2/g respectively) were determined using the standard volumetric Brunauer, Emmett, and Teller (BET) method [29]. Here, N_2 gas adsorption on the adsorbent was done at the boiling point of liquid nitrogen. A JEOL JSM 5900 LV Scanning Electron Microscopy (SEM) with Oxford INCA Energy Dispersive Spectroscopy (EDS) was used for spectral analysis. This analysis was conducted at low vacuum control pressure from the uncoated samples. The potentiometric analysis was used to obtain the Point of Zero Salt Effect (PZSE) of the PMM goethite (7.14) [30].

Synthesis of zinc oxide coated PMM goethite

A solution of zinc nitrate $(Zn(NO_3)_2.6H_2O)$ of 0.2M concentration and KOH of 0.4 M concentration were prepared with double distilled water. About 0.20 g of PMM goethite was mixed with 100 mL 1M $Zn(NO_3)_2$ solution and 180 mL of 2M KOH solution. This preparation was done to activate the PMM goethite. The activated PMM goethite was dispersed into 150 mL of 0.2M $Zn(NO_3)_2$ solution. Subsequently, about 0.4M KOH aqueous solution of three hundred microliters was titrated slowly at the rate of 1 ml^{-1} onto the content. This titration was done under vigorous stirring at ambient temperature. The formation of carbonate salt was minimized, by titrating under nitrogen flow condition, thus resulting in the formation of a white precipitate. Double distilled water was used to wash the white precipitate. The white precipitate was centrifuged and finally washed with absolute alcohol. This washing was done to free the content from NO_3^- ions. Subsequently, the solid was heated at 500℃ for 3 h in air, thus leading to the formation of zinc oxide coated goethite [31]. The PMM goethite and zinc oxide-goethite were verified through the X-ray diffraction (XRD) patterns of the products.

Batch mode adsorption experiments

To determine the effect of arsenite initial concentration, the zinc oxide coated PMM goethite suspension was made onto 50 mL and subsequently equilibrated for 24 h at pH=4-8. Here, only results at pH=4 have been reported for mimicking the scenario in hydrometallurgical contained waste. The arsenite solutions (10 mgL^{-1} to 40 mgL^{-1}) were reacted with 1% each of zinc oxide coated PMM goethite suspension. A range of solid concentrations of zinc oxide coated PMM goethite (2 gL^{-1} to 10 gL^{-1}) made onto 50 mL reacted with solutions containing arsenite ions (10 mgL^{-1}, to 40 mgL^{-1}). These were equilibrated for 24 h at pH=4-8 and the content securely sealed and kept in the dark to avoid oxidation and leaching of zinc oxide-goethite interface [32]. The adsorbent suspensions were made onto 50 mL and aged from 24-720 h. These contents were used to investigate the effect of aging. Ambient temperature was used to conduct all experiments in triplicates. To predict reaction mechanisms, kinetic experiments were conducted to elucidate the reactions involved based on the theoretical framework of existing kinetic models. The proton coefficient otherwise known as the proton exchange isotherm was derived from the change of

pH versus LogKd plot. This isotherm was based on Freundlich isotherm and the constant capacitance model [12,14] as given by equations (1, 2, 3):

$$\alpha SOH \leftrightarrow SO^- + \alpha H^- \tag{1}$$

$$logKd \leftrightarrow log(Kp\{SOH\}^\alpha) + \alpha\, pH \tag{2}$$

Here, SOH equals the mineral surface-binding site and pH equals solution pH, LogKd equals the distribution coefficient, log K_p equals the apparent equilibrium-binding constant. This constant is related to the pressure gradient in the system and was obtained by substituting the values of the equation components in (2). However, α equals the coefficient of protonation, depicting the number of protons displaced when one mole of arsenite binds to the mineral surface [12]. Proton coefficients were obtained by graphical analysis, using logKd versus pH plots. An analysis of the plot gave α, the proton coefficient as the slope. To determine this coefficient, 1% PMM zinc oxide coated goethite suspension was made onto 50 mL, reacted with Arsenite ion solution of 10 mgL^{-1} and regulated to the required pH. The content was securely sealed and kept in the dark, to avoid oxidation and leaching of zinc oxide-goethite interface. Secondly, the mass transfer rate, intraparticle diffusion and distribution coefficient, were derived from equations (3-6):

$$Q_t\,(mg/g) = [C_0 - C_t]\,V/m \tag{3}$$

Here, C_o equals the initial metal concentration (mgL^{-1}) at time t=0; C_t equals the concentration (mgL^{-1}) at time t; V equals the total zinc oxide coated goethite suspension volume and m is the weight of the sorbent (g) [12].

$$Kd = \frac{[Co - Ct]\,V/m}{Co} \tag{4}$$

Here, Kd signifies the distribution coefficient of the solute at the solid-liquid interface.

The kinetics of arsenite removal to the mineral surface binding sites was controlled by the mass transfer constant constant K_f. Here, C_t/C_o vs. time provided the slopes of the curves derived from equation (5,12):

$$\left[\frac{d\left(\frac{C_t}{C_o}\right)}{d_t}\right]_{t-0.5} \cong -K_f S_s \tag{5}$$

Here, C_t and C_0 denote the initial concentrations of arsenite at

time t, Ss equals the exposed external surface area of zinc oxide coated goethite, and K_f equals the coefficient of mass transfer. These models, as reviewed by [32,33] and derived from the Freundlich isotherm, were adopted to describe adsorption of arsenite ions. To investigate the action of intra-particle diffusion on arsenite adsorption, the Weber-Morris model was used. This model is given in equation (6):

$$Qt = K_i t^{0.5} + C \tag{6}$$

Here, K_i equals the intraparticle diffusion constant (mg/g min) and the intercept (C) represents the effect of the layer boundary. K_i values were derived from the slope of the plots of q_t vs. $t_{0.5}$. A linear plot of q_t versus $t_{0.5}$ indicated that diffusion of intraparticle was involved in the adsorption process. In addition, the rate controlling step was regulated by intraparticle diffusion, if these lines pass through the origin. Otherwise, this characteristic indicated some degree of boundary layer control. For the characterization of these reaction mechanisms, 1% zinc oxide-coated goethite was reacted with 10 mgL^{-1} arsenite solution. The content was made on 50 mL and regulated to the required pH. This was securely sealed and kept in the dark to avoid oxidation and leaching of zinc oxide-goethite interface. The amounts of arsenite ions remaining in solution were determined after 2nd h, 4th h, 6th h, 8th h, 12th h, 18th h, and 24th h. At ambient temperature, these studies were done in triplicates under reducing condition. A 0.2 µm pore size cellulose acetate filter was used on the supernatant and content analyzed for arsenite ions, using a Hitachi Atomic Absorption Spectrophotometer (HG-AAS). The percent of arsenite removed from solution was calculated from equation (7):

$$\text{Adsorption efficiency} = \left(\frac{C_0 - C_e}{C_0}\right) \times 100 \tag{7}$$

where C_0 and C_e (mgL^{-1}) are the initial and equilibrium concentrations of the arsenite in solution.

Results and Discussion

In this study, the PMM goethite contained 0.14 ppm Cu, 0.18 ppm Zn, 0.01-100.00 µm particle size range, and 1.83 % colloid. The adsorbents involved in this study have been characterized and summarized (Figures 1 and 2) and Figures 1 and 2 of supplementary information have been reported [34].

The X-ray diffraction spectrum indicated goethite as the key constituent and a combination of goethite and Zn-Oxide. The
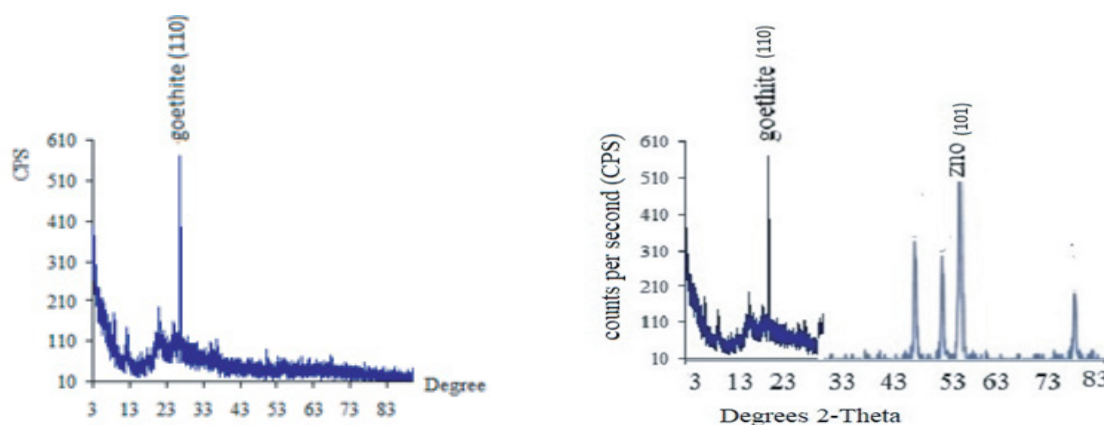

Figure 1. *X-ray diffraction. 1a) X-ray diffraction for PM4M goethite. 1b) X-jray diffraction of zinc oxide goethite composite [33].*
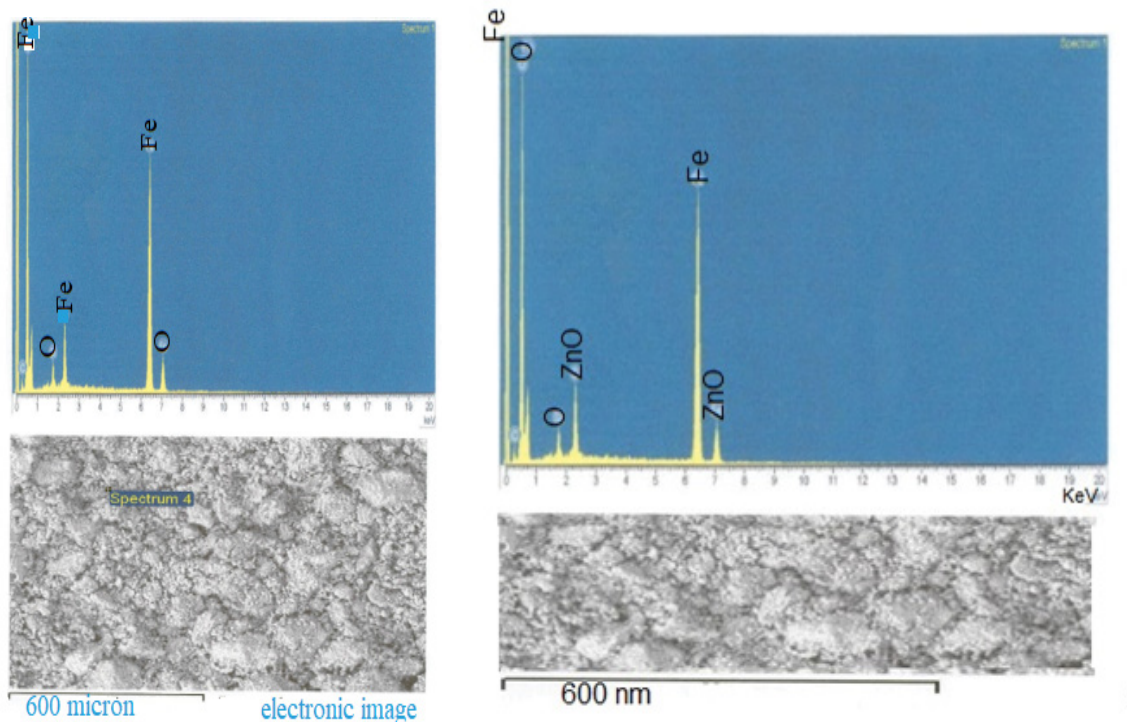
Figure 2. *EDS/SEM. a)PMM goethite showing element peaks and particle sizes. b) EDS/SEM for ZnO-PMM goethite showing element peaks and particle sizes.*
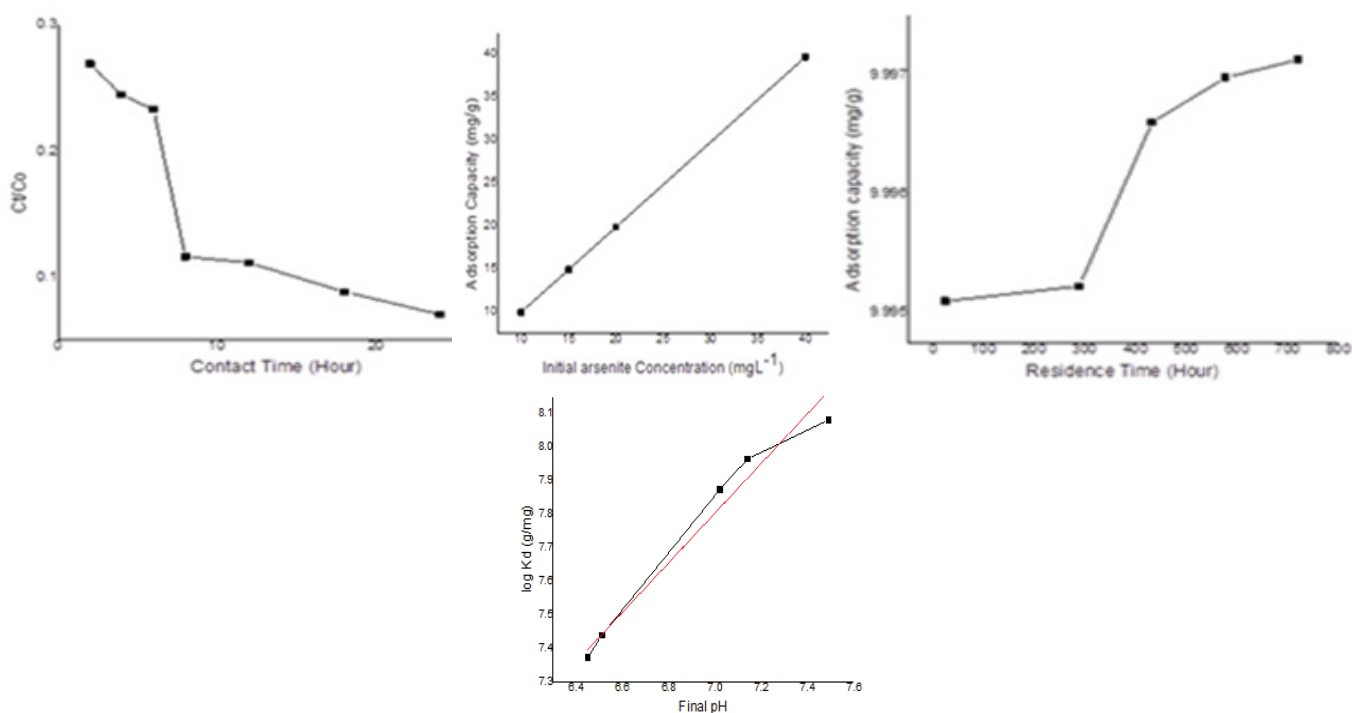

Figure 3. *a) C/C_o versus contact time. b) Adsorption capacity versus initial arsenite concentration. c) Adsorption capacity versus residence time. d) Plot of Log Kd (Distribution coefficient) versus final pH for proton coefficient.*
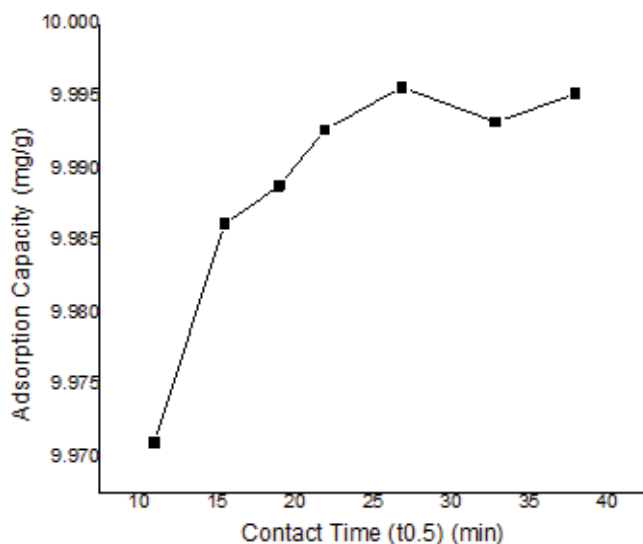
Energy Dispersive Spectroscopy (EDS) spectrum and Scanning Electron Microscopy (SEM) morphology indicated the presence of hydrous iron oxide and sulfur as trace elements. These agree with the chemical constituents of the PMM goethite and micron range values of the particle sizes (Figure 1 of Supplementary material). The point zero charge pHpzc (7.56) also was known as the point of zero salt effect and the surface area of adsorbents

are important characterization concerning adsorption (Figure 2 of Supplementary material).

Here, the total negative charges on the goethite surface equal the total positive charges. Therefore, the pHpzc determines the positive and negative charge divide on the mineral surface. The external surface area of the adsorbent controlled the quantity of exposed mineral surface available for reaction. Proton

Table 1. *Statistical presentation of proton coefficient derived from Figure 3 (Supplementary Information).*

Equation	Y=a+b*x	Value	Standard Error
Proton coefficient α	0.74		
Log Kd (mg/g)	Intercept	2.61	3.50^{-5}
	Slope	0.74	5.06^{-6}

Table 2. *Statistical presentation of intraparticle diffusion data derived from the linear fit of Figure 4 (Supplementary Information).*

Equation	Y=a+b*x	Value	Standard Error
Q_t (mgg^{-1}) min$^{0.5}$	Intercept	9.96	3.55^{-7}
	Slope	1.13^{-3}	2.37^{-4}

to remove arsenite was of arsenite ions was 93.05 % at pH=8, above the Point of Zero Charges (pHzpc) (Figure 3d).

Discussion

Reaction mechanism

The reaction mechanism was discussed based on the proton coefficient, intraparticle diffusion, and mass transfer rates. In the previous studies devoid of the zinc oxide coating, goethite displayed a proton coefficient, (α) of 0.96 [12,14]. Here, α for zinc oxide coated goethite was 0.74, less than one and slightly lower than the value recorded in the previous studies. There was an indication that protonation was lowered in the presence of zinc oxide coating. The presence of this coating could mask the acidic sites on the edges and planar surfaces of goethite. The three steps of mass transfer have been recognized in the reaction mechanism of the present study. The data tailored to Weber and Morris diffusion model exposed that adsorption progresses in three different steps. These involved: fast-external surface adsorption, and progressive slow adsorption controlled by both film diffusion and intraparticle diffusion. Although, intraparticle diffusion was involved in the adsorption process (Figure 3a and Table 2), this was not a rate-limiting reaction. Also, there was an indication of boundary layer control. In comparison with previous studies [13,14], the slope and intercept for the uncoated goethite were higher than those of the zinc oxide-goethite composite, thus suggesting that the presence of zinc oxide coating enhanced intraparticle diffusion as a near rate-limiting process. When compared with previous studies, the mass transfer rates for the coated goethite were higher than results for the bare goethite [14]. Thus, this suggested that the mass transfer of arsenite to the external layer of the zinc oxide coated goethite was enhanced (Figure 3a).

Adsorption kinetics

The adsorption of arsenite depended on the contact time. This characteristic was derived from the plot of adsorption capacity versus time (Figure 4 of supplementary information). The assessment was from 2 to 24h at ambient temperature and initial arsenite concentration of 10 mgL^{-1} at pH=4. This reaction pattern increased with an increase in contact time. The optimum adsorption was at the 24th h. The adsorption rate was initially fast, and the capacity of adsorption increased over time. This agreed with the report of other workers. However, there was no evidence of saturation of adsorption sites on the adsorbent surface. These reports were for arsenite adsorbed on porous hematite and uncoated goethite respectively. The initial quick adsorption of arsenite in the first phase may be related to the larger numbers of active adsorption sites [12].

The investigation of different arsenite concentrations was necessary since hydrometallurgical slurries and leaching muds could present different concentrations of arsenite. Here, the increase in adsorption capacity as arsenite concentration

Figure 4. *Plot of Adsorption capacity versus time for intraparticle diffusion.*

coefficient (α) was based on a theoretical framework given by equations (1,2), predicted and derived from the plot (Figure 3 of supplementary information, Table 1).

The value was 0.74, <1. The intraparticle diffusion was based on a theoretical framework given by equation (6), predicted and derived from the plot (Figure 4 of supplementary information, Table 1). The intraparticle diffusion constant derived from the slope was 1.13-3 (mg^{-1}) min$^{0.5}$ and the intercept C was 9.96, ≠ 0. This plot consisted of three linear parts with the first part representing the external mass transfer. The S-curve adsorption pattern was formed at the 19th, 22th and 38th minutes. The second and third part represented the intraparticle diffusion and adsorption inside the adsorbent surface.

The mass transfer constants (K$_f$) predicted from equations (4,5) and derived from Figure 3a are 3.61^{-6} cm^{2}hr^{-1}, 1.96^{-6} cm^2 hr^{-1}, and 1.75^{-6} cm^{2}hr^{-1} respectively. Also, this plot consisted of three linear parts with the first part higher than the second, higher than the third part. The second linear part started after the 6th h and the third linear part started after the 8th h. Figure 3b consisted of a single linear part. There was an increase in capacity of adsorption as arsenite initial concentration was increased. The adsorption capacity increased from 9.92 to 39.73 mg^{-1} over the range of arsenite concentration investigated. Contact time i.e. aging increased with increase in adsorption capacity. (Figure 3c) This plot consisted of three linear parts. The S-curve adsorption pattern was formed at the 288th and 432nd h. (Figure 3c). The maximum adsorption capacity was 9.99 mg/g at the 720th h. Adsorption efficiency generally increased with increase in pH. In acidic medium, the adsorption capacity was low but increased with increase in pH (Figure 3c). As predicted from equation 7, the efficiency of the zinc oxide-goethite composite

increased, suggested that the mass transfer rate of arsenite ions between the solid-solution divide was not controlled by concentration pressure gradient (Figure 3c). This characteristic was different from the reports of Akpomie et al., [34]. In both cases, there was reported a decrease in the adsorption capacity for some heavy metals adsorbed on montmorillonite (100 to 300 mgL^{-1}). In addition, there was a linear decrease in adsorption of arsenite on uncoated goethite. In this report, the constant linear plot indicated a unified increase in capacity of adsorption due to the non-saturation of the active and reactive sites.

In this report, the increase in adsorption capacity as aging was increased depicted an S-curve pattern adsorption mechanism (Figure 3d). This characteristic was different from the report provided in [13] for arsenite adsorbed on uncoated goethite over the same range of aging. Over there, there was a reported complex decrease in adsorption pattern linked to an outer sphere, inner sphere complexation, and intraparticle diffusion. In this report, the higher magnitude of S-curve adsorption pattern was essentially controlled by hydrolysis, reactive support of zinc oxide coating and an increase in the reorganization of active sites.

The effect of pH on arsenite adsorption

The investigation of the pH effect was necessary, given that arsenite removal was pH dependent. As pH was increased, protonation and hydroxylation of zinc oxide-goethite interface controlled the adsorption process. This characteristic was different from the report of [13] in the absence of zinc oxide coating. In that case, there was a complex decrease in adsorption as pH was increased outside the point of zero charges. Here, the surface charges on the zinc oxide coated goethite surface affected the role of solution pH. The point of zero charges (pHzpc) of goethite was approximately 7.56. Below this pHzpc value, goethite was positively charged and arsenite was negatively charged. As the pH was increased around the point of zero charges, there was a decrease in protonation and enhancement in hydroxylation, thus favoring arsenite adsorption. In addition, the stability of zinc oxide is in the pH range of more than 7, and the optimum adsorption of arsenite was expected above pH 7 as reported elsewhere [35].

Conclusion

The synthesis of zinc oxide coated MM goethite was done and the characterization conducted using usual laboratory techniques. The batch mode technique was used to test the adsorption of arsenite on the zinc oxide coated PMM goethite. The mechanism of reaction tested included: proton coefficient that was less than one, an intraparticle diffusion that was controlled by the boundary layer, and some mass transfer rates that were higher than those of barely coated goethite. There was a linear increase in adsorption capacity as arsenite concentration was increased. Thus, the active and reactive sites of the PMM zinc oxide coated goethite was not yet saturated. The adsorption of arsenite was increased by aging. The maximum adsorption of arsenite was 9.99 mg^{-1}. The higher magnitude of S-curve adsorption pattern was essentially controlled by hydrolysis and increased reorganization of active sites of the zinc oxide coating. The increase in pH led to protonation and hydroxylation of zinc oxide coated goethite. These characteristics controlled the adsorption process. Herein, the adsorption efficiency maximized

at 93.05%. Therefore, increasing the pH led to a decrease in protonation and enhancement in hydroxylation. Subsequently, this increase in pH led to an increase in the adsorption of arsenite. Therefore, the zinc oxide coating enhanced the reorganization of active and reactive sites on the goethite external surface. This coating promoted the adsorption of arsenite.

Acknowledgment

Disclosure Statement

No potential conflict of interest was reported by the authors.

References

1. Srivastava S, Verma PC, Chaudhry V, et al. Influence of inoculation of arsenic-resistant Staphylococcus arlettae on growth and arsenic uptake in *Brassica juncea* (L.) Czern. Var. R-46. J Hazard Mater. 2013;262:1039-47.

2. Lin L, Qiu W, Wang D, et al. Arsenic removal in aqueous solution by a novel Fe-Mn modified biochar composite: Characterization and mechanism. Ecotoxicol Environ Saf. 2017;144:514-21.

3. Wu K, Zhang N, Liu T, et al. Competitive adsorption behaviors of arsenite and fluoride onto manganese-aluminum binary adsorbents. Colloids Surf A Physicochem Eng Asp. 2017;529:185-94.

4. Han X, Song J, Li YL, et al. As (III) removal and speciation of Fe (Oxyhydr) oxides during simultaneous oxidation of As (III) and Fe (II). Chemosphere. 2016;147:337-44.

5. Aktar S, Jahan M, Alam S, et al. Individual and combined effects of arsenic and lead on behavioral and biochemical changes in mice. Biol Trace Elem Res. 2017;177(2):288-96.

6. Han DS, Song JK, Batchelor B, et al. Removal of arsenite (As (III)) and arsenate (As (V)) by synthetic pyrite (FeS_2): Synthesis, the effect of contact time, and sorption/desorption envelopes. J Colloid Interface Sci. 2013;392:311-8.

7. Zhang M, Gao B, Varnoosfaderani S, et al. Preparation and characterization of novel magnetic biochar for arsenic removal. Bioresour Technol. 2013;130:457-62.

8. Nahar N, Rahman A, Ghosh S, et al. Functional studies of AtACR2 gene putatively involved in accumulation, reduction and/or sequestration of arsenic species in plants. Biologia. 2017;72(5):520-6.

9. Jain CK, Ali I. Arsenic: occurrence, toxicity and speciation techniques. Water Res. 2000;34(17):4304-12.

10. Boddu VM, Abburi K, Talbott JL, et al. Removal of arsenic (III) and arsenic (V) from aqueous medium using chitosan-coated biosorbent. Water Res. 2008;42(3):633-42.

11. Misstear B, Banks D, Clark L. Water wells and boreholes. John Wiley Sons. 2017.

12. Egirani DE, Baker AR, Andrews JE. Arsenite removal from

aqueous solution by mixed mineral systems I. Reactivity and removal kinetics. Int J Recent Sci Res. 2013;4(4).

13. Egirani DE, Baker AR, Andrews JE. Arsenite removal from aqueous solution by mixed mineral systems II. the role of solution composition and ageing. Int J Recent Sci Res. 2013;4(4):439-43.

14. Egirani DE, Andrews JE, Baker AR. Arsenite removal from aqueous solution using mixed mineral systems injected with iron sulfide under sulfidic-anoxic conditions 1: Reactivity and removal kinetics. J Environ Sci, Toxicol Food Technol. 2014;3:893-910.

15. Egirani DE, Andrews JE, Baker AR. Arsenic removal from aqueous solution using mixed mineral systems injected with sphalerite under sulfidic-Anoxic conditions II. The role of solution composition and aging. J Environ Sci, Toxicol Food Technol. 2014;3:881-92.

16. Egirani DE, Wessey N, Aderogba A. Effect of mineral systems injected with zinc sulfide on arsenite removal from aqueous solution: Part II. American J Applied Chemistry. 2015;3:201-6.

17. Egirani DE, Wessey N. Effect of clay and goethite mineral systems inoculated with pyrite on arsenite removal from aqueous solution. J Chem Metal. 2016;51(6):735-46.

18. Garelick H, Jones H, Dybowska A, et al. Arsenic pollution sources. InReviews of Environmental Contamination Volume 197 2009 (pp. 17-60). Springer, New York, NY.

19. Plescia P, Maccari D. Recovering metals from red mud by thermal treatment and magnetic separation. Jom. 1996; 48(1):25-8.

20. Van der Sloot HA. Systematic leaching behavior of trace elements from construction materials and waste materials. J Environ Sci. 1991;48:9-36.

21. Masscheleyn PH, Delaune RD, Patrick Jr WH. Effect of redox potential and pH on arsenic speciation and solubility in contaminated soil. Environ Sci Technol. 1991;25(8):1414-9.

22. Devi RR, Umlong IM, Das B, et al. Removal of iron and arsenic (III) from drinking water using iron oxide-coated sand and limestone. Appl Water Sci. 2014;4(2):175-82.

23. Mohan D, Pittman Jr CU. Arsenic removal from water/ wastewater using adsorbents-a critical review. J Hazard Mater. 2007;142(1-2):1-53.

24. Sahmoune MN. The Role of biosorbents in the removal of arsenic from water. Chem Eng Technol. 2016;39(9):1617-28.

25. Yoon Y, Zheng M, Ahn YT, et al. Synthesis of magnetite/ non-oxidative graphene composites and their application for arsenic removal. Sep Purif Technol. 2017;178:40-8.

26. Gray PJ, Tanabe CK, Ebeler SE, et al. A fast and fit-for-purpose arsenic speciation method for wine and rice. J Anal At Spectrom. 2017;32(5):1031-4.

27. Guo X, Jin X, Zhao X, et al. Nano-adsorptive effects manifested in arsenite adsorption onto the nano-sized goethite. Sci Adv Mater. 2014;6(4):793-802.

28. Jiuhui QU. Research progress of novel adsorption processes in water purification: a review. J Environ Sci. 2008;20(1):1-3.

29. Wei S, Tan W, Liu F, et al. Surface properties and phosphate adsorption of binary systems containing goethite and kaolinite. Geoderma. 2014;213:478-84.

30. Ghorbani HR, Mehr FP, Pazoki H, et al. Synthesis of ZnO nanoparticles by precipitation method. Orient J Chem. 2015;31(2):1219-21.

31. Romero M, Rincón JM. Surface and bulk crystallization of glass-ceramic in the Na_2O-CaO-ZnO-PbO-Fe_2O_3-Al_2O_3-SiO_2 system derived from a goethite waste. J Am Ceram Soc. 1999;82(5):1313-7.

32. Bandpei AM, Mohseni SM, Sheikhmohammadi A, et al. Optimization of arsenite removal by adsorption onto organically modified montmorillonite clay: Experimental and theoretical approaches. Korean J Chem Eng. 2017;34(2):376-83.

33. Egirani DE, Poyi NR, Wessey N, et al. Synthesis and characterization of goethite coated with copper oxide and its effect on the removal of aqueous mercury (II) ions. J Taibah Univ Sci. 2018;12(5):652-60.

34. Akpomie KG, Dawodu FA, Adebowale KO. The mechanism on the sorption of heavy metals from binary-solution by low cost montmorillonite and its desorption potential. Alexandria Eng J. 2015;54(3):757-67.

35. Samad A, Furukawa M, Katsumata H, et al. Photocatalytic oxidation and simultaneous removal of arsenite with CuO/ZnO photocatalyst. J Photochem Photobiol. 2016;325:97-103.

*Correspondence to:

Egirani DE
Niger Delta University, Wilberforce Island
Nigeria
E-Mail: eenonidavidson@yahoo.com
ORCID iD: 0000-0002-4067-3117